Nicotinamide adenine dinucleotide fluorescence spectroscopy and imaging of isolated cardiac myocytes

John Eng, Ronald M. Lynch, and Robert S. Balaban
Laboratory of Cardiac Energetics, National Heart, Lung and Blood Institute, Bethesda, Maryland 20892

ABSTRACT Nicotinamide adenine dinucleotide (NADH) plays a critical role in oxidative phosphorylation as the primary source of reducing equivalents to the respiratory chain. Using a modified fluorescence microscope, we have obtained spectra and images of the blue autofluorescence from single rat cardiac myocytes. The optical setup permitted rapid acquisition of fluorescence emission spectra (390–595 nm) or intensified digital video images of individual myocytes. The spectra showed a broad fluorescence centered at 447 ± 0.2 nm, consistent with mitochondrial NADH. Addition of cyanide resulted in a 100 ± 10% increase in fluorescence, while the uncoupler FCCP resulted in a 82 ± 4% decrease. These two transitions were consistent with mitochondrial NADH and implied that the myocytes were 44 ± 6% reduced under the resting control conditions. Intracellular fluorescent structures were observed that correlated with the distribution of a mitochondrial selective fluorescent probe (DASPMI), the mitochondrial distribution seen in published electron micrographs, and a metabolic digital subtraction image of the cyanide fluorescence transition. These data are consistent with the notion that the blue autofluorescence of rat cardiac myocytes originates from mitochondrial NADH.

INTRODUCTION

Mitochondrial reduced nicotinamide adenine dinucleotide (NADH) is the primary electron source for the electron transport chain in oxidative phosphorylation. It is currently believed that the mitochondrial NADH/NAD^+ redox state may be a primary control site in cellular respiration (1,2,3), so that measurement of the cellular NADH redox state and its compartmentation is critical toward developing an understanding of metabolic regulation in the intact cell.

Cellular NADH (reduced) and NAD^+ (oxidized) levels have been measured using enzymatic assays on tissue extracts. The determination of the NADH and NAD^+ compartmentation has relied on the measurement of specific redox couples participating in localized enzymatic reactions, such as the lactate dehydrogenase system in the cytosol (4) and the glutamate dehydrogenase system in the mitochondrial matrix (5). Surface fluorescence has been used to measure the relative level of NADH in both perfused (3) and *in vivo* tissues (6). NADH absorbs ultraviolet light with a maximum at 340 nm and emits a broad-band blue fluorescence centered at ~ 450 nm. Oxidized nicotinamide adenine dinucleotide (NAD^+) does not absorb or fluoresce significantly at these wavelengths. Data from biochemical determinations show that the blue fluorescence observed in the heart originates primarily from bound NADH and reduced nicotinamide adenine dinucleotide phosphate (NADPH) in the mitochondria, with insignificant contributions from free cytosolic NADH and NADPH (7). In isolated heart mitochondria, NADH is the predominant reduced pyridine nucleotide (8) and has as much as a fourfold greater fluorescence yield than NADPH (9).

In contrast to biochemical determinations, the monitoring of NADH autofluorescence provides a rapid, nondestructive measure of relative NADH levels and allows each experimental sample to act as its own control. Using fluorescence techniques, it has also been possible to characterize the NADH distribution of subcellular mitochondrial aggregates in intact cells (10,11).

The purpose here was to characterize the blue autofluorescence of single rat cardiac myocytes using microspectrophotometry and video microscopy techniques. The blue autofluorescence was characterized by analyzing its fluorescence emission spectrum, its response to known inhibitors of oxidative phosporylation, and its topological distribution within the cell. The single-cell preparation eliminates a number of problems accompanying whole-heart preparations: organ motion, cell environment inhomogeneity, and inner filter effects from tissue and blood chromophores—such as hemoglobin, myoglobin, and cytochromes that can alter the spectral characteristics of the fluorescence signal.

Preliminary results of this work were presented at the Biophysical Society Meeting, Phoenix, AZ, USA (1988).

Dr. Lynch's present address is Department of Physiology, University of Massachusetts, Worcester, MA 01605.

METHODS AND MATERIALS

Materials

Collagenase (type 2) was purchased from Worthington Biochemical Co. Freehold, NJ; lot 67040M; bovine serum albumin (BSA, fraction V; lot 349) was from Miles Laboratories, Inc., Naperville, IL. Calcium-free Minimum Essential Medium (MEM) was prepared locally (National Institutes of Health Media Unit lots EVS80025 and EVS80064). The respiratory uncoupler carbonylcyanide-*p*-trifluoromethoxy phenylhydrazone (FCCP) was obtained from Boehringer-Mannheim Diagnostics Inc., Mannheim, F.R.G. The fluorescent dyes 5(and 6)-carboxy fluorescein diacetate, succinimidyl ester, and 2-(4-dimethyl aminostyryl)-*N*-methylpyridinium iodide (DASPMI) were obtained from Molecular Probes, Inc. Eugene, OR. Glassware in contact with the isolated myocytes was siliconized with Sigmacote (Sigma Chemical Co., St. Louis, MO).

Preparation of cardiac myocytes

Calcium-tolerant cardiac myocytes were prepared according to a method modified from that of Montini et al. (12). Adult Sprague-Dawley rats (200–300 g) were anesthetized by intraperitoneal injection of 1.0 g sodium pentobarbital (Richmond Vetinary Supply Co., Richmond, VA). Concomitantly, 1,500 U heparin sodium (Elkins-Sinn, Inc., Cherry Hill, NJ) was injected intraperitoneally to inhibit blood coagulation. Hearts were quickly excised and mounted on an apparatus for Langendorff retrograde perfusion (13). The hearts were perfused with 30–40 ml calcium-free MEM (solution A) at 8 ml/min to remove blood. Solution A was then replaced with 100 ml solution B (1 mg/ml collagenase and 1 mg/ml BSA in solution A). Perfusion was maintained at 8 ml/min for 22 min while recirculating the solution B. All solutions were maintained at pH 7.4 and 37°C while bubbling with 95% O_2-5% CO_2. The BSA in solution B is believed to protect cell membranes by binding fatty acids which may cause membrane disruption through a detergent action (14).

The ventricular tissue was diced to 2 mm pieces, added to 10 ml solution B in a small siliconized flask, and placed in an orbital shaker (90 rpm, 25 mm orbit). After 10 min of shaking, 10 ml solution C (1 mg/ml BSA in solution A) were added to the flask, and the supernatant cell suspension was poured into a siliconized centrifuge tube. This suspension was centrifuged at low speed (~30 *g*, 45 s), resuspended and centrifuged in 10 ml solution C, resuspended and sedimented (5–6 min) in 5 ml solution C, and finally resuspended in 5 ml solution C. This process was repeated for the remaining tissue fragments in the flask, after additional 10 min shaking cycles, until a majority of the myocytes were dispersed.

The collagen-coated superfusion chamber was loaded with 20–40 ml of the final cell suspension. The cells were allowed to settle and adhere to the chamber bottom. For all experiments, the myocytes in the chamber were constantly superfused at 3 ml/min with a pH 7.4 buffer solution containing Hepes (10 mM), glucose (10 mM), NaCl (120 mM), KCl (4.7 mM), KH_2PO_4 (1 mM), $MgSO_4$ (1 mM), $NaHCO_3$ (24 mM), creatine (1 mM), and taurine (1 mM) (solution D). The superfusate was equilibrated under room air and maintained at 37°C. For the single-cell spectroscopy experiments, the superfusate also contained 1 mM $CaCl_2$.

Optical apparatus

The superfusion chamber was mounted on a modified inverted microscope (Nikon, Inc. Instrument Div., Garden City, NY) (Fig. 1 and reference 15). Fluorescence excitation light from a 100 W mercury arc lamp (Nikon, Inc.) was controlled by a computer-actuated electronic shutter, passed through a 360 nm bandpass filter (transmission 330–380 nm), reflected by a dichroic mirror (reflectance 420 nm), and focused on an individual cardiac myocyte by a 63× Neofluar; Carl Zeiss Inc., Thornwood, NY (oil immersion, NA 1.25) objective lens. The 360 nm fluorescence excitation filter was used for all experiments. Fluorescence emission light from the entire field of view was transmitted by the dichroic mirror to reach ocular objectives, a diffraction grating monochromator, an image intensifier screen, or a 35 mm film camera.

Oxygen consumption

Oxygen consumption (QO_2) was determined using a Clarke-type O_2 electrode (Yellow Springs Instrument, Yellow Springs, OH) mounted in a 1 ml stirred chamber maintained at 37°C. The electrode was calibrated with air-equilibrated solution C.

Spectroscopy

The monochromator (Instruments SA, Inc., Metuchen, NJ) output spectrum was imaged by a silicon intensified target (SIT) camera (model 1254; Princeton Applied Research, Princeton, NJ). With this arrangement, a 390–595 nm spectrum was dispersed over 500 camera pixels in the horizontal direction, providing a spectral resolution of 0.4 nm/pixel horizontally. The SIT camera scanning was controlled by a multichannel controller (model 1216; Princeton Applied Research) interfaced to a DEC 11/23 MINC minicomputer (Digital Equipment Corp., Marlboro, MA). The 1216 controller was programmed to sum the SIT camera pixels in the vertical direction and send the resulting string of 500 values to the minicomputer, where these values were digitized by analog to digital converters. A single 390–595 nm fluorescence emission spectrum was obtained in one 33 ms SIT scan. To improve signal-to-noise, 10 SIT scans were summed to obtain each data acquisition. Each data acquisition was corrected for the camera dark

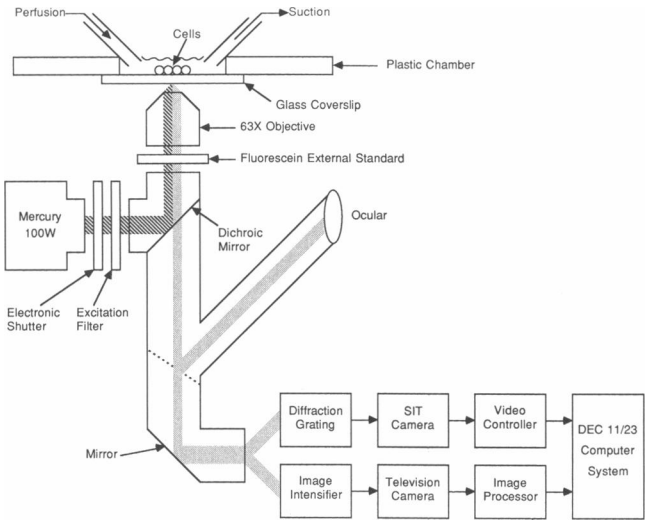

FIGURE 1 Rapid scanning microspectrofluorometer designed for acquiring fluorescence emission spectra from single cells at video framing rates. ▧ represents excitation light that is reflected onto the sample by the dichroic mirror. □ represents the single-cell fluorescence emission, which is transmitted by the dichroic mirror. The fluorescence emission could also be diverted to an intensified digital video image acquisition system or to a photographic film camera (not shown).

current by digitally subtracting 10 SIT scans acquired with the excitation shutter closed. The total UV light exposure was ~ 830 ms (500 ms for shutter opening).

All fluorescence emission spectra were corrected for background field fluorescence using least squares fitting of the raw spectrum to a reference function. The reference function was the sum of two spectra: a corrected autofluorescence spectrum from a single myocyte (used for all corrections) and a spectrum taken from a cell-free area near each experimental myocyte. Fitting the raw spectrum to the sum of these two reference spectra enabled the cellular autofluorescence signal to be separated from fluorescence originating from background sources (e.g., optics, perfusate). The background also included fluorescence originating from an aqueous fluorescein solution which was placed in the optical pathway to act as an external standard during spectroscopic acquisitions. This external fluorescence standard was used to correct for light source and detector fluctuations. After least squares fitting of each raw spectrum, the intensity of the fluorescence peak originating from the external standard was used to scale each spectrum to a standard intensity. Since fluorescence from the external standard was part of the background, it was properly separated from cellular autofluorescence by the least squares fitting routine.

All spectra were Fourier filtered to 20 complex harmonics. Computer software for spectral data acquisition, storage, and analysis was written in BASIC and is available from the authors upon request. All values are reported as the mean ± standard error of the mean.

Imaging

The microchannel image intensifier (Newport Corp., Fountain Valley, CA) output image was coupled to a television camera. The television image was digitized and manipulated by an image processing system (IP-512 series; Imaging Technology, Inc., Woburn, MA) interfaced to the DEC computer. Each pixel in the final digitized image represented a resolution of 0.2 μm × 0.2 μm × 256 grayscale levels.

Fluorescence emission images were acquired by the image processor as a sum of ten consecutive 33-ms video frames. The television camera's dark current signal was found to be negligible. The digitized video images were processed and stored on the DEC computer system.

RESULTS

Cell viability and spectral characteristics

Viable myocytes were defined as those cells possessing rod-shaped morphology and maintaining striated structural integrity (Fig. 2). Other methods of determining cell viability, such as trypan blue stain exclusion, electrical stimulation, and ATP levels, have been used on similarly prepared myocytes (16), but these methods have no clear advantage over simple morphological criteria.

FIGURE 2 Brightfield photomicrograph of a typical rod-shaped, viable cardiac myocyte isolated as described in Methods. Included for comparison in this photomicrograph is a rounded, nonviable myocyte that was apparently damaged during the isolation procedure. This photograph was made from a 1/4-s exposure (effective aperture $f/6.7$) on Kodak Ektachrome color reversal film (ISO 200). For all photographs in this presentation, no corrections were made for the spectral sensitivity of the photographic film.

The difference in viability was also evident with fluorescence excitation, under which the rod-shaped, viable myocytes emitted a relatively bright blue fluorescence, while the rounded, nonviable myocytes emitted a relatively dim green fluorescence (Fig. 3). These two patterns of fluorescence are also contrasted in the autofluorescence emission spectra obtained from the individual myocytes (Fig. 4). The residual green fluorescence probably originates from mitochondrial oxidized flavoproteins, which have a fluorescence maximum at 510 nm (17).

The single-cell blue autofluorescence spectrum (Fig. 4) had a maximum intensity at 447 ± 0.2 nm ($n = 10$), which is consistent with NADH of a mitochondrial origin (18,19). To further correlate the single-cell spectrum with a mitochondrial origin, a suspension of rat heart mitochondria was studied using the same optical setup and identical data acquisition parameters as for the single-cell experiments. The fluorescence emission spectrum collected from the mitochondria had a maximum intensity at 455 nm (Fig. 5), which is similar to the single-cell autofluorescence spectrum. The rat heart mitochondria were isolated using standard methods (20).

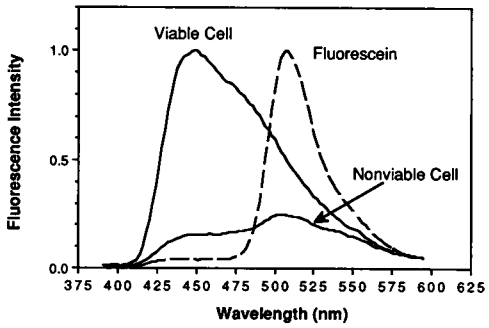

FIGURE 4 Autofluorescence emission spectra under 366 nm UV excitation comparing the blue autofluorescence of a viable myocyte with the low-intensity autofluorescence of a nonviable myocyte. The fluorescence emission spectrum of a fluorescein solution (used as an external standard) does not overlap with the blue autofluorescence maximum.

Metabolic correlations

To further investigate the correlation with mitochondrial NADH, simple metabolic transitions were performed to change the myocytes' mitochondrial NADH/NAD^+

FIGURE 3 Autofluorescence emission photomicrograph of the cells shown in Fig. 2 under 366 nm UV excitation (30-s exposure, effective aperture $f/6.7$, Ektachrome 200 film).

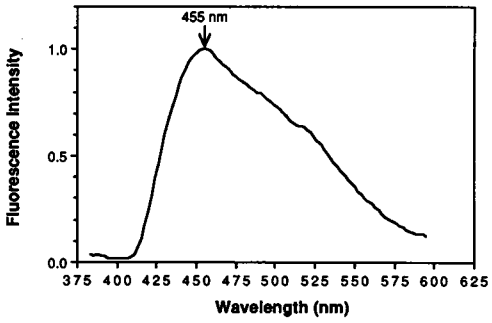

FIGURE 5 Autofluorescence emission spectrum of isolated rat heart mitochondria collected using the same apparatus as shown in Fig. 1. Data acquisition parameters were identical to those used for the individual myocytes.

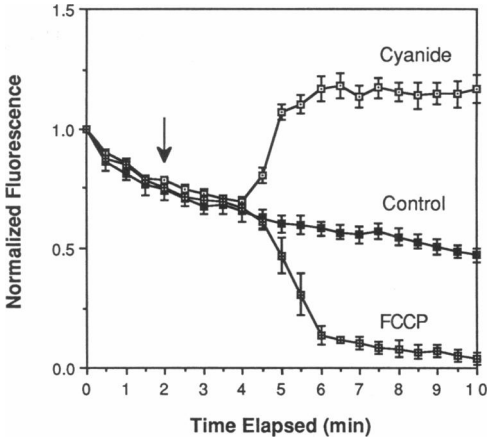

FIGURE 7 Timecourse plot of the metabolic transitions. Each data point represents the intensity at the blue autofluorescence maximum (447 nm) at the given point in time. All intensities are normalized to the initial value at 0 min. The arrow indicates addition of cyanide or FCCP. The delay in response after the arrow was due to the dead space in the chamber perfusion apparatus.

redox state. Cyanide is an electron transport inhibitor that blocks NADH oxidation, increasing the mitochondrial NADH/NAD$^+$ ratio (more reduced state). Adding 400 μM cyanide to the superfusate resulted in an increase in the blue autofluorescence signal intensity (Fig. 6 *A*). This transition is consistent with an increase in mitochondrial NADH as a result of cyanide's effect as an electron transport inhibitor. The timecourse of this transition (Fig. 7) shows an intensity increase of 2.0 ± 0.1 times control after 5 min.

To oxidize the NADH/NAD$^+$ redox couple, FCCP was added to the superfusion medium. FCCP is a mitochondrial uncoupler that stimulates NADH oxidation, decreasing the mitochondrial NADH/NAD$^+$ ratio (more oxidized state). Adding 2 μM FCCP to the superfusion medium resulted in a decrease in the NADH autofluorescence signal intensity (Fig. 6 *B*). This transition is consistent with a decrease in mitochondrial NADH as a result of FCCP's effect as a mitochondrial uncoupler. Fluorescence signal from 2 μM FCCP in the superfusate was insignificant with this apparatus. The timecourse of the transition (Fig. 7) demonstrates an intensity decrease of 0.18 ± 0.04 times control after 5 min. Assuming that FCCP caused maximal oxidation and that cyanide caused maximal reduction, the control cells in this preparation were 44 ± 6% reduced.

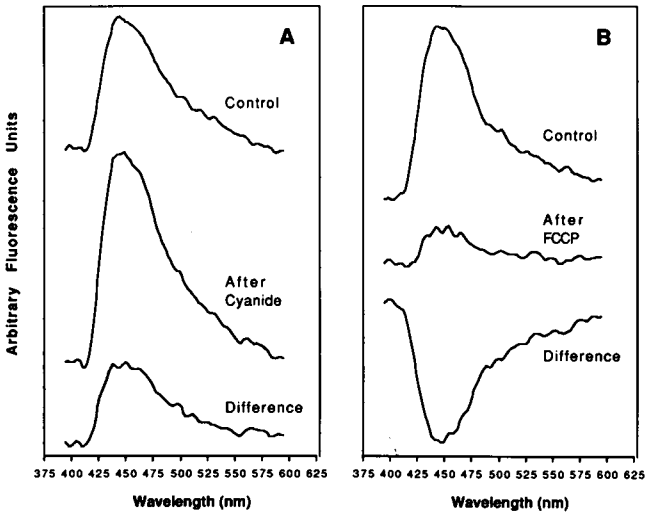

FIGURE 6 Fluorescence emission spectra for the cyanide (A) and FCCP (B) transitions. The top spectrum of each set was acquired during a control period. The middle spectra were acquired 5 min after adding cyanide (A) or FCCP (B) to the surrounding medium. The bottom spectra are difference spectra (middle minus top).

As seen in the timecourse plots (Fig. 7), a consistent decrease in the fluorescence signal was observed during the control period. The magnitude of this phenomenon was independent of the metabolic substrates supplied to the cell, but was dependent on the frequency of the cell's exposure to UV light. Based on these characteristics, the fluorescence decrease was attributed to photobleaching of a component of the autofluorescence. Due to its consistent behavior, this fluorescent component did not significantly affect analysis of the metabolically labile fluorescence component.

To see if the effect of an increase in cytosolic NADH could be detected, lactate was added to the superfusate. Lactate increases the cytosolic NADH/NAD$^+$ ratio through the lactate dehydrogenase reaction. However, addition of 5 mM lactate resulted in no significant change (n = 3) in the blue autofluorescence of the isolated myocytes. Epinephrine (10^{-7} M), acetate (2 mM), and excess calcium (~2.5 mM) are less specific effectors of the

mitochondrial NADH/NAD^+ redox state. Experiments involving the addition of these substances also demonstrated no significant changes ($n = 3$ each) in the blue autofluorescence emission intensity from these myocytes.

Topological correlations

A pattern of longitudinal stripes was observed in the blue autofluorescence of these myocytes (Fig. 3); these stripes suggested a mitochondrial origin. To investigate this possibility, the fluorescent mitochondrial dye DASPMI was added to the perfusion chamber. DASPMI is a fluorescent dye that preferentially partitions into the mitochondria (21). When DASPMI in dimethylsulfoxide was added to the perfusion chamber (approximate final concentration of 4 μg/ml), stripes of fluorescence attributed to the dye were observed in the viable myocytes (Fig. 8). The stripes of fluorescence observed in the DASPMI-treated myocytes were similar in distribution to those of the native blue autofluorescence (Fig. 3).

The metabolic significance of these fluorescent stripes was examined by obtaining a digitized video image of an individual myocyte in the presence of cyanide (400 μM) and digitally subtracting a video image of the same myocyte taken before adding the cyanide (Fig. 9). The presence of the fluorescent stripes in the digital subtraction image is evidence that we are observing fluorescence from the metabolically active pool of NADH.

An alternate interpretation of the native autofluorescence striped pattern was that the observed pattern represented diffraction, interference, or absorption caused by the cellular contents, especially the numerous contractile elements which also run longitudinally. To examine this possibility, the spatial distribution of carboxyfluorescein, a fluorescent probe that uniformly distributes throughout the cytosol, was analyzed. Carboxyfluorescein fluoresces only after it has been taken up and hydrolyzed by cytosolic esterases. When carboxyfluorescein in dimethylsulfoxide was added to the perfusion chamber (approximate final concentration of 10 μg/ml), the fluorescence was uniformly distributed within each viable myocyte, and no fluorescence striped pattern was observed (Fig. 10). This observation suggests that the striped pattern seen in the native blue autofluorescence

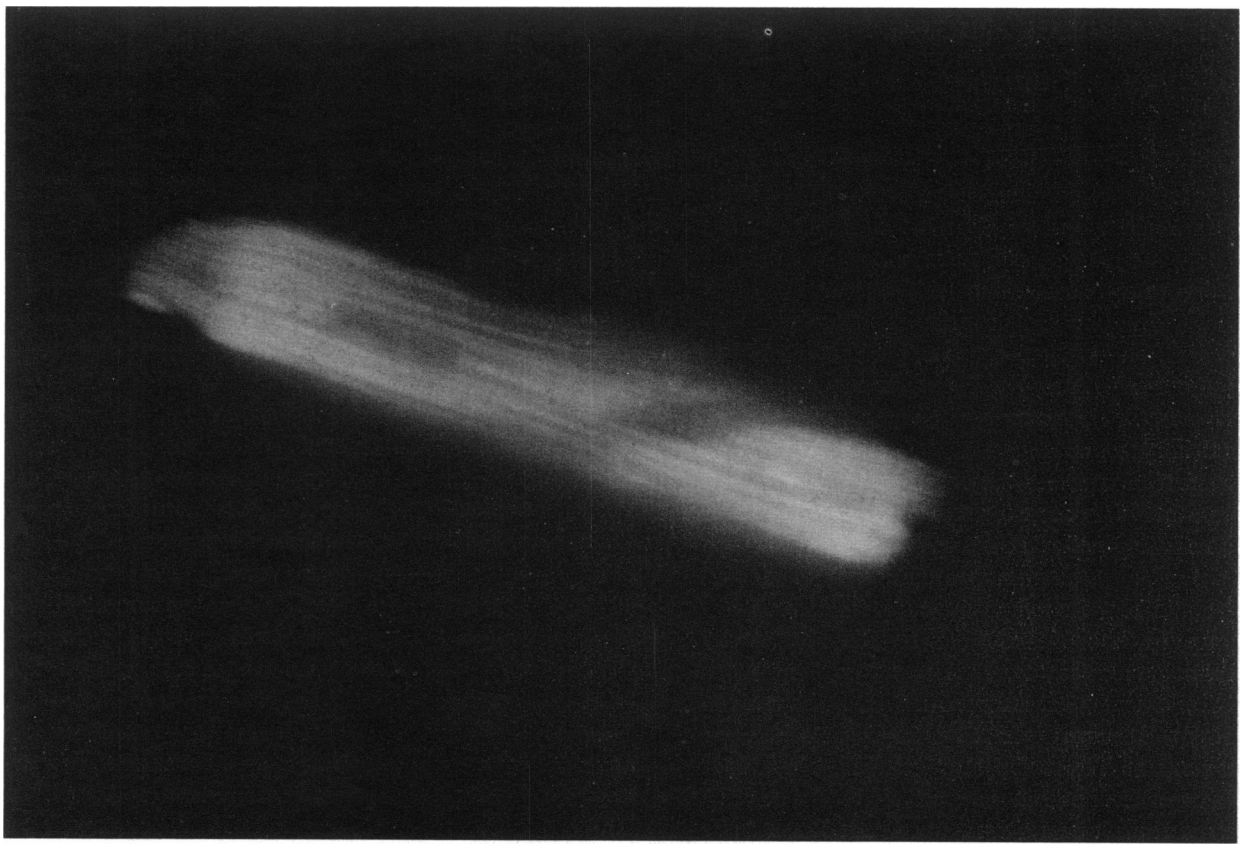

FIGURE 8 Autofluorescence photomicrograph of a mycocyte that has taken up DASPMI, a mitochondrial selective fluorescent probe (15-s exposure, effective aperture $f/6.7$, Ektachrome 200 film, printed black and white). The actual color of the fluorescence shown in this black and white photograph is yellow-white, consistent with the DASPMI fluorescence emission maximum at 556 nm (21).

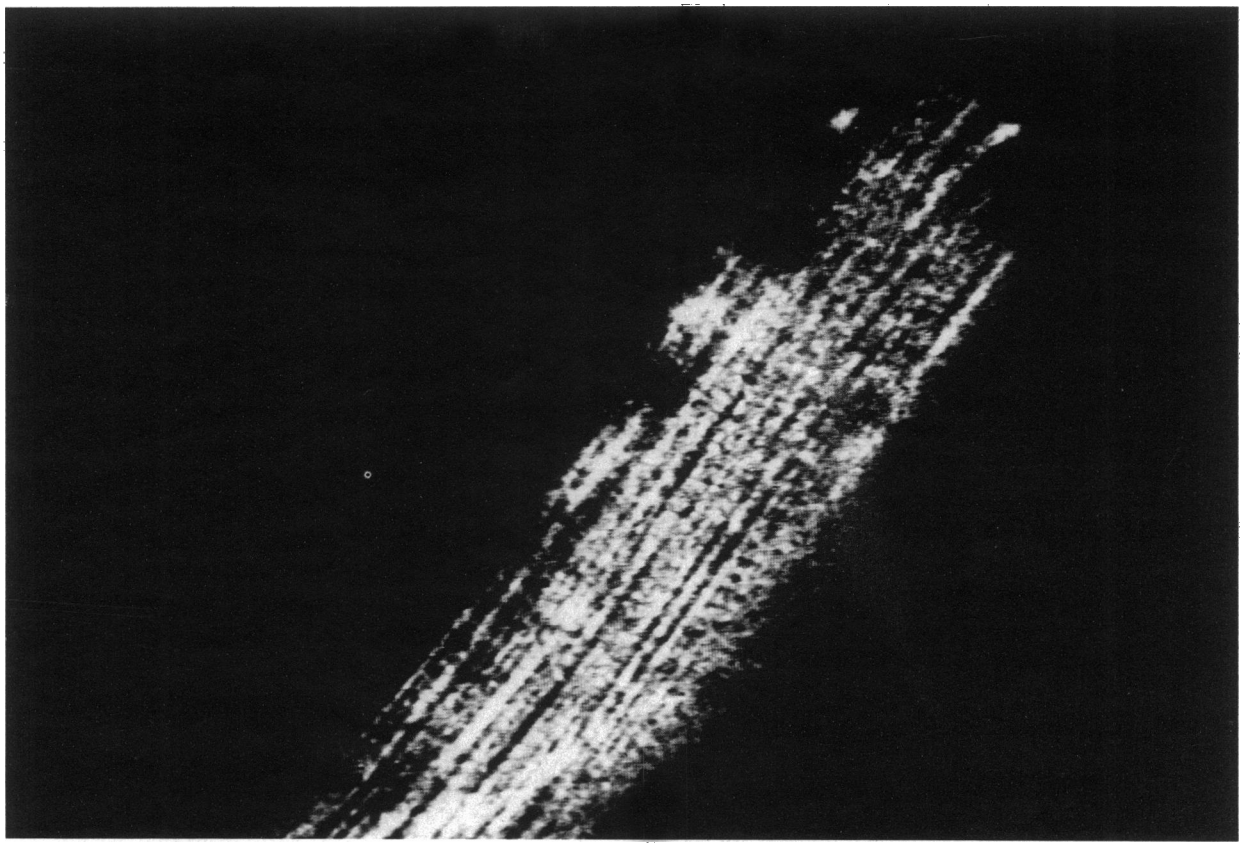

FIGURE 9 Digital subtraction image that shows where the blue fluorescence increases after adding cyanide to a single myocyte.

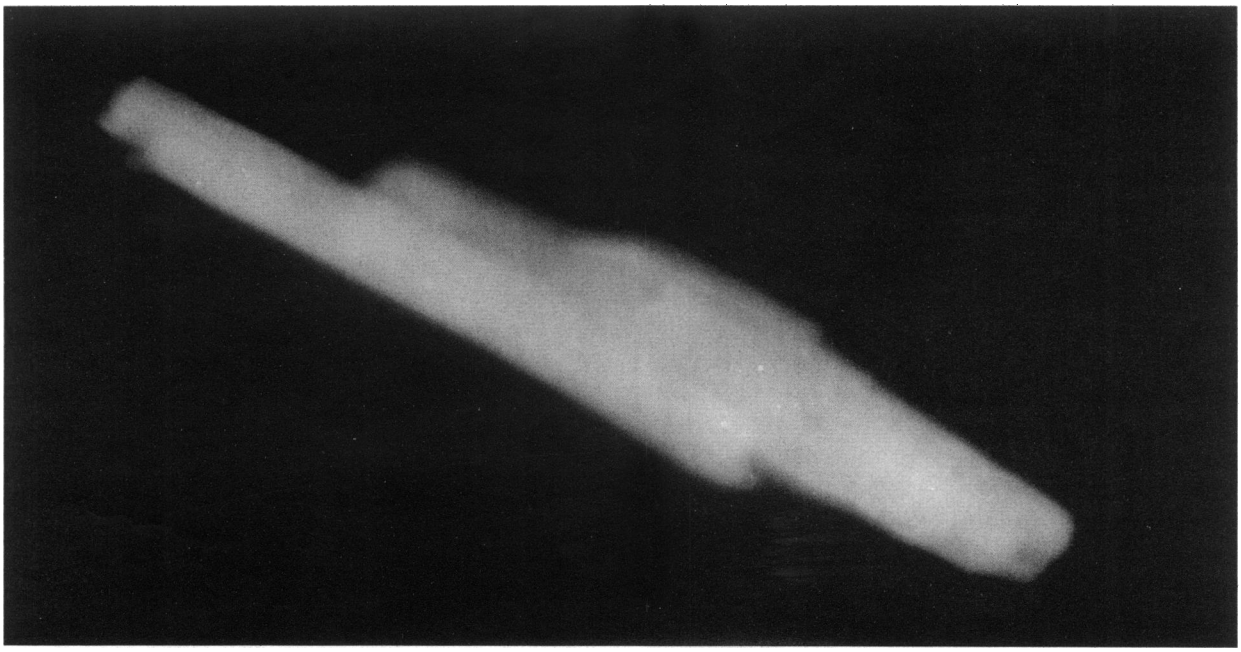

FIGURE 10 Autofluorescence photomicrograph of a myocyte that has taken up carboxyfluorescein, a fluorescent dye that uniformly distributes throughout the cytoplasm (4-s exposure, effective aperture $f/6.7$, Ektachrome 200 film, printed black and white).

(Fig. 3) represents true structural distribution and not simply a diffraction or interference pattern caused by the cellular contents.

Oxygen consumption

The absence of a significant NADH redox change with epinephrine or Ca^{2+} suggested that the cells may be in a quiescent state, with low ATP turnover via oxidative phosphorylation. To examine this possibility, the respiratory state of these myocytes was evaluated by measuring oxygen consumption of a cell suspension. The cells were isolated by methods identical to the single-cell studies and suspended in the same solution D at 37°C. Addition of epinephrine or Ca^{2+} produced little or no effect on the respiration of the suspended cells, while FCCP-uncoupling increased respiration 5.1 ± 0.6 times control. These results indicate that electron transport in the mitochondria of the control cells was well coupled to ATP synthesis and that the mitochondria were not responsive to extracellular Ca^{2+}. The control cells were respiring at only 20% of the maximum respiratory rate, assuming the maximum respiratory rate is the uncoupled rate.

DISCUSSION

Fluorescence emission is an established method for monitoring the NADH redox state of various tissues and mitochondrial suspensions. For meaningful interpretation of such studies, it has been important to establish the subcellular origin of the detected fluorescence. In the perfused rat heart, studies have demonstrated a linear correlation between NADH fluorescence and the total NADH content determined biochemically (22). More recent studies have shown a linear correlation between NADH fluorescence and the free mitochondrial NADH/NAD^+ ratio determined from the analysis of glutamate dehydrogenase substrates (7).

Here, we present evidence that the blue autofluorescence detected from single myocytes originates predominantly from mitochondrial NADH. This conclusion was based on the spectral characteristics, metabolic responsiveness, and topological distribution of the blue autofluorescence within a single cell. The fluorescence emission spectrum from the single rat myocyte has a maximum at 447 nm, which is consistent with the NADH fluorescence spectrum collected from rat heart mitochondria in the same apparatus (Fig. 5). Similar NADH fluorescence spectra have been reported in rat liver mitochondria (18,19). By comparison, pure NADH has a fluorescence maximum at 440 nm when bound to lactate dehydrogenase and 465 nm when in aqueous solution (23). In studies of intact tissues and organs, the maximum fluorescence emission is observed at longer wavelengths, but this has been attributed to quenching of the fluorescence emission by myoglobin (24). This shift in wavelength was not observed in the single-cell fluorescence spectrum, indicating that myoglobin absorption was negligible as a result of the short optical path lengths in this preparation.

The single-cell fluorescence responded to cyanide and FCCP in a manner consistent with the action of these drugs on mitochondrial NADH metabolism. The addition of lactate, which should increase the cytosolic NADH/NAD^+ ratio, caused no significant change in the fluorescence signal, indicating that the cytosolic NADH does not contribute significantly to the fluorescence signal. This observation is consistent with the finding that the myocardial lactate/pyruvate (L/P) ratio does not correlate with NADH surface fluorescence (7).

Finally, the single-cell fluorescence was not uniformly distributed throughout the cell, but was concentrated in longitudinal stripes. The spacing and orientation of these fluorescent stripes corresponds to the ultrastructural distribution of mitochondria as shown by electron microscopy of similarly prepared myocytes (Fig. 11 and reference 25).

Taken together, these data indicate that the blue autofluorescence from single rat myocytes originates from mitochondrial NADH. Quantitation of the mitochondrial NADH/NAD^+ ratio from this NADH fluorescence signal requires that fully reduced and fully oxidized NADH fluorescence levels be established for the individual myocyte. Here, cyanide additions were used to estimate the maximally reduced NADH fluorescence signal, and FCCP additions were used to estimate the fully oxidized condition. The complete oxidation of NAD^+ by uncouplers has been uncertain since it was found that in renal cells, NADH oxidation by uncouplers depended on the particular substrate(s) present (26). Here, however, the FCCP-uncoupled condition was considered to represent complete oxidation because the fluorescence signal with FCCP treatment was so low (0.10 ± 0.02 in absolute fluorescence units) compared with the fully reduced cyanide condition (1.14 ± 0.04 fluorescence units). Therefore, in the worst case, the fully oxidized fluorescence signal could only be overestimated by 10%, which was the magnitude of the blue autofluorescence remaining after FCCP.

From the cyanide and FCCP fluorescence transitions, we estimate that mitochondrial NAD^+ in these myocytes is ~44% reduced under control conditons. This NADH redox state approximates that of actively respiring isolated mitochondria in State 3 (27), where NAD^+ is 53% reduced. Furthermore, increases in NADH fluorescence, ranging from 1.7- to 2.6-fold, have been observed in the isolated glucose perfused heart during transitions from normoxia to hypoxia (3, 22, 28). However, biochemical

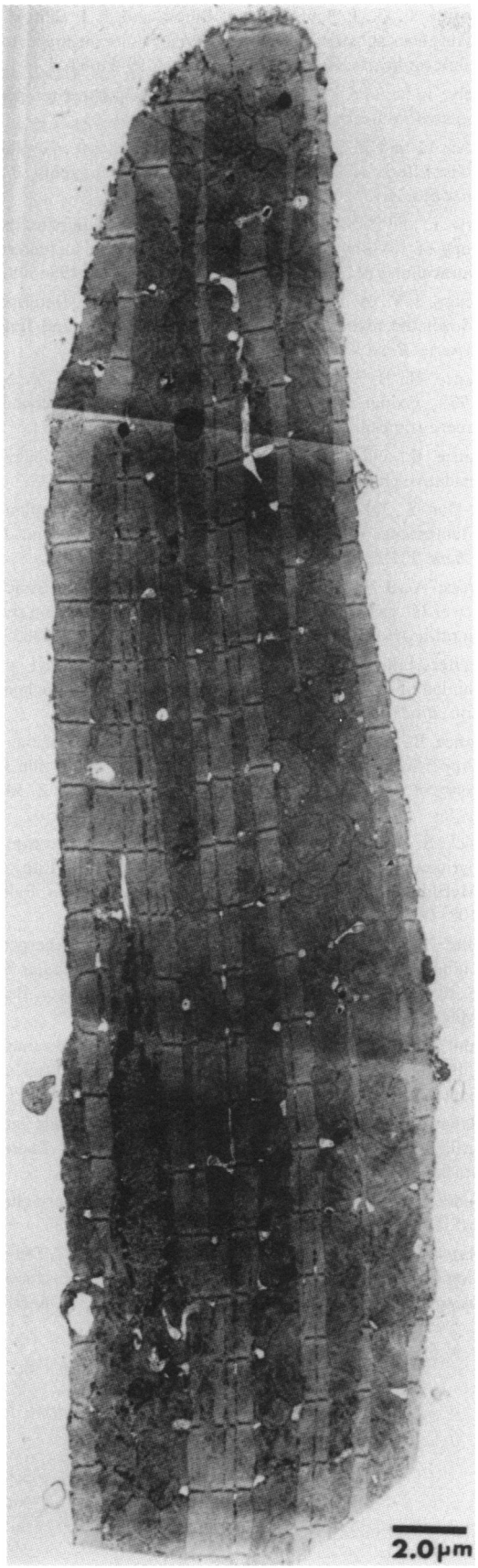

analysis of the glutamate dehydrogenase system in the isolated glucose perfused heart has shown that the free mitochondrial NADH/NAD^+ ratio in anoxia is 4–6 times the ratio in normoxia (5, 7). These data would predict a 4- to 6-fold NADH fluorescence increase for the transition from control to fully reduced, compared with the only twofold NADH fluorescence increase observed in studies of perfused tissue (3, 22, 28). One reason for this apparent discrepancy is that biochemical methods measure free NADH and NAD^+, while fluorescence measurements involve primarily the bound pool of mitochondrial NADH (7). Because mitochondrial NADH fluorescence is greatly enhanced by protein binding (9, 23), a change in fluorescence can be interpreted as a change in the redox state of bound NAD or a change in the binding or physical environment of each NADH molecule. With the present data, we cannot discern which interpretation (perhaps both) is a more accurate description of the changes that are occurring. However, it is interesting to consider that the regulation of the NADH/NAD^+ redox state or its free energy may involve changes in the physical binding properties for mitochondrial NADH.

Even though the mitochondrial NADH redox state estimated here was similar to that of actively respiring mitochondria, the respiratory studies on the isolated myocytes indicated that these cells were turning over ATP at only 20% of V_{max} and would therefore be considered quite inactive. The low rate of oxidative phosphorylation in these cells was not due to substrate limitations since addition of lactate or acetate did not increase respiration or change the NADH redox state, unlike previous studies on metabolically active renal cells (26). The myocytes in this preparation contracted only infrequently in the presence of calcium. Even when the myocytes did contract, little work was performed by myosin ATPase because contraction occurred against no mechanical load. Because myosin ATPase represents the myocytes' major ATPase activity, it is reasonable to presume that ATP consumption and ADP production by these cells was limited by a low ATP turnover by myosin ATPase. Thus, under the conditions here, the myocytes were relatively quiescent, operating well below their maximum capacity for oxidative phosphorylation due to limited ATP hydrolysis by myosin ATPase.

In summary, spectroscopic, metabolic, and topologic evidence have been presented that establishes a mitochondrial origin for the blue autofluorescence of individual

FIGURE 11 Electron micrograph montage of longitudinal sections taken of a rat cardiac myocyte isolated by standard procedures. Stripes of mitochondria are clearly seen along the cell's length. (Reproduced by permission from reference 25.)

cardiac myocytes. This preparation allows topological monitoring of metabolism in a single cell and will enable further study of the compartmentation of cardiac metabolic regulation at the single cell level.

John Eng is a Howard Hughes Medical Institute National Institutes of Health research scholar.

Received for publication 9 August 1988 and in final form 7 November 1988.

REFERENCES

1. Denton, R. M., and J. G. McCormack. 1980. On the role of the calcium transport cycle in heart and other mammalian mitochondria. *FEBS (Fed. Eur. Biochem. Soc.) Lett.* 119:1–8.
2. Hansford, R. G. 1985. Relation between mitochondrial calcium transport and control of energy metabolism. *Rev. Physiol. Biochem. Pharmacol.* 102:1–72.
3. Katz, L. A., A. P. Koretsky, and R. S. Balaban. 1987. Respiratory control in the glucose perfused heart: A ^{31}P NMR and NADH fluorescence study. *FEBS (Fed. Eur. Biochem. Soc.) Lett.* 221:270–276.
4. Bücher, T., and M. Klingenberg. 1958. Wege des Wasserstoffs in der lebendigen Organisation. *Angew. Chem.* 70:552–570.
5. Nuutinen, E. M., J. K. Hiltunen, and I. E. Hassinen. 1981. The glutamate dehydrogenase system and the redox state of mitochondrial free nicotinamide adenine dinucleotide in myocardium. *FEBS (Fed. Eur. Biochem. Soc.) Lett.* 128:356–360.
6. Chance, B., P. Cohen, F. Jobsis, and B. Schoener. 1962. Intracellular oxidation-reduction states in vivo. *Science (Wash. DC).* 137:499–508.
7. Nuutinen, E. M. 1984. Subcellular origin of the surface fluorescence of reduced nicotinamide nucleotides in the isolated perfused rat heart. *Basic Res. Cardiol.* 79:49–58.
8. Klingenberg, M., W. Slenczka, and E. Ritt. 1959. Vergleichende biochemie der pyridinnucleotid-systeme in mitochondrien verschiedener organe. *Biochem. Z.* 332:47–66.
9. Estabrook, R. W. 1962. Fluorometric measurement of reduced pyridine nucleotide in cellular and subcellular particles. *Anal. Biochem.* 4:231–245.
10. Chance, B., and B. Thorell. 1959. Localization and kinetics of reduced pyridine nucleotide in living cells by microfluorometry. *J. Biol. Chem.* 234:3044–3050.
11. Kohen, E. 1964. Pyridine nucleotide compartmentalization in glass-grown ascites cells. *Exp. Cell Res.* 35:303–316.
12. Montini, J., G. J. Bagby, A. H. Burns, and J. J. Spitzer. 1981. Exogenous substrate utilization in Ca^{2+}-tolerant myocytes from adult rat hearts. *Am. J. Physiol.* 240:H659–H663.
13. Neely, J. R., and M. J. Roveto. 1975. Techniques for perfusing isolated rat hearts. *Methods Enzymol.* 39:43–63.
14. Bihler, I., and B. Jeanrenaud. 1970. ATP content of isolated fat cells: Effects of insulin, ouabain, and lipolytic agents. *Biochim. Biophys. Acta.* 202:496–506.
15. Kurtz, I., and R. S. Balaban. 1985. Fluorescence emission spectroscopy of 1,4-dihydroxyphthalonitrile: a method for determining intracellular pH in cultured cells. *Biophys. J.* 48:499–508.
16. Cheung, J. Y., A. Leaf, and J. V. Bonventre. 1985. Determination of isolated myocyte viability: staining methods and functional criteria. *Basic Res. Cardiol.* 80(Suppl.):23–30.
17. Chance, B., B. Schoener, R. Oshino, F. Itshak, and Y. Nakase. 1979. Oxidation-reduction ratio studies of mitochondria in freeze-trapped samples. *J. Biol. Chem.* 254:4764–4771.
18. Chance, B., and H. Baltscheffsky. 1958. Respiratory enzymes in oxidative phosphorylation. *J. Biol. Chem.* 233:736–739.
19. Avi-Dor, Y., J. M. Olson, M. D. Doherty, and N. O. Kaplan. 1962. Fluorescence of pyridine nucleotides in mitochondria. *J. Biol. Chem.* 237:2377–2383.
20. Vercesi, A., B. Reynafarje, and A. L. Lehninger. 1978. Stoichiometry of H^+ ejection and Ca^{2+} uptake coupled to electron transport in rat heart mitochondria. *J. Biol. Chem.* 253:6379–6385.
21. Bereiter-Hahn, J. 1976. Dimethylaminostyrylmethyl pyridiniumiodine (DASPMI) as a fluorescent probe for mitochondria in situ. *Biochim. Biophys. Acta.* 423:1–14.
22. Chance, B., J. R. Williamson, D. Jamieson, and B. Schoener. 1965. Properties and kinetics of reduced pyridine nucleotide fluorescence of the isolated and in vivo rat heart. *Biochem. Z.* 341:357–377.
23. Velick, S. F. 1961. Spectra and structure in enzyme complexes of pyridine and flavine nucleotides. *In* Light and Life. W. D. McElroy and B. Glass, editors. Johns Hopkins Press, Baltimore. 108–143.
24. Gibbs, C. L., and J. B. Chapman. 1979. Cardiac energetics. *In* Handbook of Physiology, Section 2: The Cardiovascular System. S. R. Geiger, editor. American Physiological Society, Bethesda, Maryland. Vol. I. Chap. 22:775–804.
25. Frank, J. S., A. J. Brady, S. Farnsworth, and G. Mottino. 1986. Ultrastructure and function of isolated myocytes after calcium depletion and repletion. *Am. J. Physiol.* 250:H265–H275.
26. Balaban, R. S., and L. J. Mandel. 1988. Metabolic substrate utilization by rabbit proximal tubule: an NADH fluorescence study. *Am. J. Physiol.* 254:F407–F416.
27. Chance, B., and G. R. Williams. 1956. The respiratory chain and oxidative phosphorylation. *Adv. Enzymol.* 17:65–134.
28. Koretsky, A. P., L. A. Katz, and R. S. Balaban. 1987. Determination of pyridine nucleotide fluorescence from the perfused heart using an internal standard. *Am. J. Physiol.* 253:H856–H862.